

TRANSFORMER RATIO MEASUREMENTS FROM RAMPED BEAMS IN THE PLASMA BLOWOUT REGIME USING EMITTANCE EXCHANGE

R. Roussel*, G. Andonian, W. Lynn, J. Rosenzweig, UCLA, 90095 Los Angeles, USA
 J. Power, M. Conde, S. Doran, G. Ha, J. Seok, E. Wisniewski, C. Whiteford,
 Argonne National Laboratory, 60439, Lemont, USA

Abstract

We present initial measurements from a UCLA-Argonne Wakefield Accelerator collaborative plasma wakefield acceleration (PWFA) experiment aimed at demonstrating the dependence of transformer ratio on longitudinal beam shape. The transformer ratio or the ratio between the maximum acceleration of the witness and the maximum deceleration of the drive beam, is key to a efficient, beam-based, plasma wakefield accelerator design. Utilizing the unique capabilities of the emittance exchange (EEX) beamline, we may obtain transformer ratios approaching the theoretical limit in PWFA. We present the experimental beamline design, relevant beam diagnostics and explore preservation of the longitudinal beam profile.

TRANSFORMER RATIO FOR PWFA

The development of beam based plasma wakefield acceleration (PWFA) schemes has provided a potential path for miniaturization of large scale accelerators, due to plasma's ability to sustain accelerating gradients in excess of 10 GeV/m [1, 2]. While this provides a substantial improvement over current state of the art accelerating schemes, practical realization of an accelerator based solely on PWFA requires further improvement of efficient transfer of energy.

One critical figure of merit that requires investigation is known as the transformer ratio (TR). In a collinear wakefield scheme the transformer ratio is defined as $TR = |W_+|/|W_-|$, the ratio between the maximum accelerating field that a witness bunch would experience and the maximum decelerating field that the drive would experience.

As a direct result from the Fundamental Theory of Beam Loading, Bane. et. al. showed that longitudinally symmetric drive beams have a maximum TR of 2 [3]. Further study suggested that using a longitudinal ramp in bunch current could increase the TR to $N\pi$ where N is the ramp length in characteristic wakefield wavelengths [4]. A further increase in transformer ratio could be attained by adding a small "doorstep" or "double-triangle" feature at the beginning of the ramp. Until recently it has been difficult to create these longitudinal distributions in a precise manner, but the recent development of pulse stacking [5, 6] and emittance exchange [7] methods have started to allow detailed study of this effect in collinear accelerator schemes [8, 9]. We present experimental work using emittance exchange to create and sample high transformer ratio wakefields in a single stage PWFA accelerator.

* roussel@ucla.edu

EXPERIMENTS AT THE ARGONNE WAKEFIELD ACCELERATOR

The Argonne Wakefield Accelerator facility at Argonne National Laboratory is the ideal test-bed for exploring wakefield effects from longitudinally shaped beams. A cesium telluride cathode based photoinjector was used to inject a 12 nC beam into the drive beamline consisting of 4 L-band, normal conducting accelerating cavities. The resulting beam, with the parameters listed in Table 1, is then sent into the Emittance Exchange beamline (see Fig. 1) to shape the beam longitudinally. A tungsten mask was first used to shape the beam profile transversely. The emittance exchange process [7] is then used to transform the transverse distribution into a longitudinal one, creating a drive-witness pair.

Table 1: Design Beam Parameters

Parameter	Value	Unit
Energy	40	MeV
Drive Charge	1.0	nC
Drive Length	4	mm
Witness Charge	0.4	nC
Witness Length	4	mm
$\epsilon_{n,x}$	~800	mm.mrad

Two masks were developed to test different drive profiles. Both masks were designed to accept a uniform transverse beam distribution created by a laser spot from a micro-lens array on the photocathode [10]. The first mask was designed to produce a single triangle drive bunch, whose length was matched to span two plasma wavelengths (see Table 2 for plasma parameters) along with a low charge, equal length witness bunch to sample the wakefield. The second mask was designed to create a double triangle like feature at the head of the drive profile with a similar witness. This consisted of a single triangle as before, but with an added ramp in the first quarter wavelength of the main triangle. These profiles have theoretical transformer ratios of $N\pi$ and $\sqrt{1 + (2\pi N - 1)^2}$ respectively [11], where N is the length of the main ramp in terms of plasma wavelengths. With the mask designs used it should be possible to achieve a $TR > 2$ for these advanced shapes.

After shaping, the beam was then transported into the experimental beamline. A hollow cathode arc plasma source [12] was used to produce a plasma with the parameters seen in Table 2. Due to stringent vacuum requirements of CsTe cathode operation ($P \approx 10^{-10}$ Torr), the plasma source chamber ($P \approx 10^{-2}$ Torr) was separated from the rest of the beam-

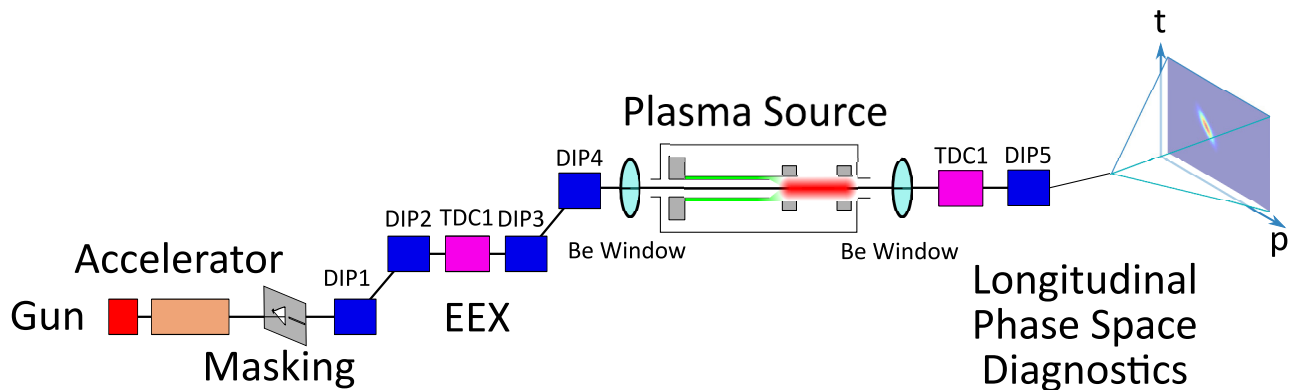


Figure 1: Overview schematic of the beamline at AWA showing the drive linac, emittance exchange beamline and experimental beamline including dipoles (DIP), transverse deflecting cavities (TDC) and Beryllium windows.

line using 125 μm thick Beryllium windows on either side. Quadrupole triplets were used to focus the beam at the window locations to reduce emittance growth from multiple scattering [13]. After on-line optimization the normalized beam emittance going into the plasma source was estimated to be on the order of 0.5-1 mm.rad and 0.4 mm.rad after the second Be window (due to the significant particle loss at the plasma source).

Table 2: Hollow Cathode Arc Plasma Parameters

Parameter	Value	Unit
Plasma Density	0.3 - 1.5 $\times 10^{14}$	cm^{-3}
Plasma Wavelength	6.1 - 2.7	mm
Plasma Length	60	mm
Plasma Width	8	mm
Neutral Gas Pressure	50	mTorr
Discharge Duration	0.2	ms

Optical transition radiation was used to measure the beam size at the plasma interaction point. This beam size diagnostic consisted of a silver plated dielectric mirror that was inserted into the beam path using a motorized actuator. The mirror was inserted at a 45° angle with respect from the beam axis and imaged using a CCD camera. The dielectric substrate for the mirror also emitted a detectable amount of Cherenkov light, which enabled coarse beam alignment before focusing was enabled. To protect the mirror surface quality, the mirror was shielded from the plasma during discharges using an aluminum shield. The rms transverse size of the beam was 0.9 mm x 0.5 mm in the horizontal and vertical direction respectively.

The longitudinal phase space diagnostic consisted of a slit, transverse deflecting cavity, and a rectangular dipole [14]. The L-band (1.3 GHz) cavity provided a longitudinally dependant deflecting force on the beam with a measured strength parameter of $\kappa = 1.84 \text{ m}^{-1}$. A dipole with a measured peak field of 0.14 T and a magnetic length $L = 0.365 \text{ m}$ provides a 20° bend such that the dispersion at a downstream YAG is $\eta = 0.312 \text{ m}$. A horizontal slit with a width

of 100 μm was used to collimate the beam vertically in order to increase the timing resolution of the measurement by reducing the vertical emittance. This had the added benefit of preventing off axis particles from receiving a longitudinal energy kick from the transverse deflecting cavity, which could possibly blur wakefield energy gain.

LONGITUDINAL DISTRIBUTION EVOLUTION

Optimization of the longitudinal beam profile delivered from the EEX has been the subject of intense study [7] as the transformer ratio is highly sensitive to the quality of the linear ramp and the subsequent tail. To maintain the optimal profile through the experimental beamline, simulation codes OPAL [15] and elegant [16] were used to perform beamline optimization. The beam is given a positive longitudinal energy chirp due to the emittance exchange process. This results in chromatic aberrations which limits strong focusing of the beam. The beam also retains a strong longitudinal correlation with the vertical direction (Fig. 2a) as no transformations happen to coordinates not in the EEX bend plane. The need for strong focusing at both the Be windows and at the plasma interaction point causes this correlation to distort the longitudinal beam profile. Off axis particles have longer travel paths than core particles in the case of strong focusing, which causes them to lag behind. For the mask designs shown here, this effect is felt by the particles at the end of the ramp, which contributes to the growth of a tail (Fig. 2b).

This effect is mitigated by reducing the beam size in the vertical direction throughout the experimental beamline. The profile continues to develop a tail at each focus location, which includes both Be windows, the plasma source and the final longitudinal diagnostics. Given this, is expected that the profile at the plasma source has a smaller tail than the measured profile at the longitudinal diagnostic (Fig. 3). The longitudinal projection shows a significant difference relative to the idealized profile with a significant tail. This is primarily due to the effects described previously and not due to vertical emittance growth as the beam has been collimated in that direction. The beam centroid also retains its

Content from this work may be used under the terms of the CC BY 3.0 licence (© 2019). Any distribution of this work must maintain attribution to the author(s), title of the work, publisher, and DOI

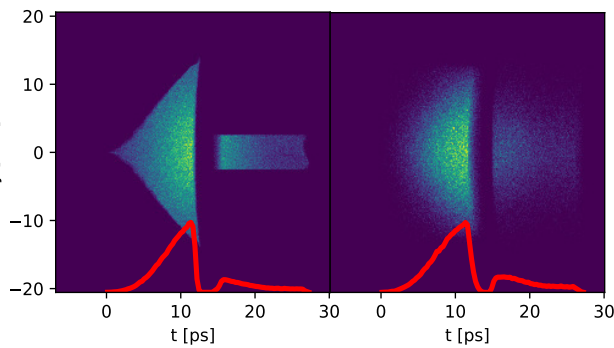


Figure 2: Simulated vertical cross section of the beam at (a) the exit of the EEX beamline and (b) after the plasma interaction point. Red lines show the beam distribution projected onto the temporal axis (beams travel to the left).

longitudinal energy chirp from the EEX process. The bump seen the slice energy centroid at approx. 25 ps is further evidence of particle slippage from inside the ramp profile, as these particles have a higher energy than a linear chirp would suggest, which would imply that they were earlier in the distribution when the chirp was applied.

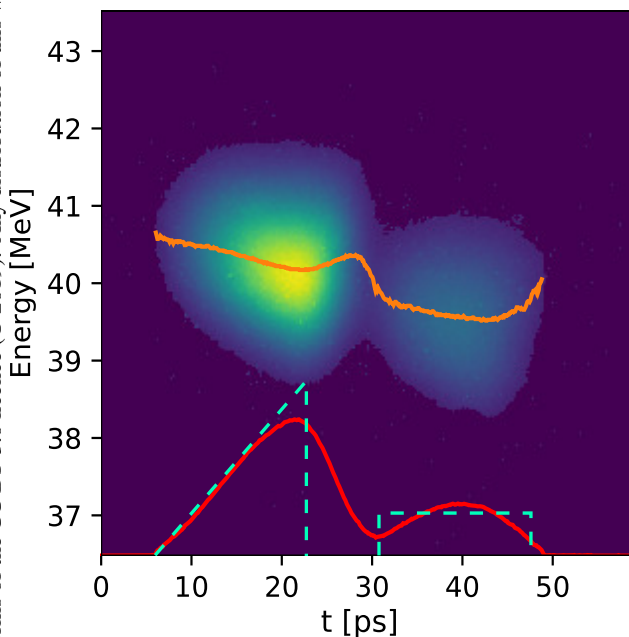


Figure 3: Measured longitudinal phase space after the experimental beamline. The temporal slice energy centroid (orange line), temporal projection (red line) and idealized temporal profile (green dashed line) is also plotted.

CONCLUSION

This paper serves as an overview of the experimental parameters used for an experiment regarding the transformer ratio due to ramped beams in the plasma blowout regime. A consideration of the beam dynamics through the experimental beamline was discussed, with maintaining the longitudinal profile through multiple beam waists as a central focus.

Preliminary longitudinal phase space measurements were also shown and are consistent with simulations.

ACKNOWLEDGEMENTS

This work was supported by DOE contract DE-SC0017648 and the DOE SCGSR fellowship.

REFERENCES

- [1] I. Blumenfeld *et al.*, “Energy doubling of 42 GeV electrons in a metre-scale plasma wakefield accelerator,” *en, Nature*, vol. 445, no. 7129, pp. 741–744, Feb. 2007, issn: 1476-4687. doi: 10.1038/nature05538. <https://www.nature.com/articles/nature05538>
- [2] M. Litos *et al.*, “High-efficiency acceleration of an electron beam in a plasma wakefield accelerator,” *en, Nature*, vol. 515, no. 7525, pp. 92–95, Nov. 2014, issn: 1476-4687. doi: 10.1038/nature13882. <https://www.nature.com/articles/nature13882>
- [3] K. L. F. Bane, P. B. Wilson, and T. Weiland, “Wake fields and wake field acceleration,” *en, in AIP Conference Proceedings*, vol. 127, AIP, 1985, pp. 875–928. doi: 10.1063/1.35182. <http://aip.scitation.org/doi/abs/10.1063/1.35182>
- [4] K. L. F. Bane, P. Chent, and P. B. Wilson, *On Collinear Wake Field Acceleration*.
- [5] C. Jing *et al.*, “Increasing the transformer ratio at the Argonne wakefield accelerator,” *Phys. Rev. ST Accel. Beams*, vol. 14, no. 2, p. 021302, Feb. 2011. doi: 10.1103/PhysRevSTAB.14.021302. <https://link.aps.org/doi/10.1103/PhysRevSTAB.14.021302>
- [6] G. Loisch *et al.*, “Photocathode laser based bunch shaping for high transformer ratio plasma wakefield acceleration,” *Nuclear Instruments and Methods in Physics Research Section A: Accelerators, Spectrometers, Detectors and Associated Equipment*, 3rd European Advanced Accelerator Concepts workshop (EAAC2017), vol. 909, pp. 107–110, Nov. 2018, issn: 0168-9002. doi: 10.1016/j.nima.2018.02.043. <http://www.sciencedirect.com/science/article/pii/S0168900218301979>
- [7] G. Ha *et al.*, “Precision Control of the Electron Longitudinal Bunch Shape Using an Emittance-Exchange Beam Line,” *Phys. Rev. Lett.*, vol. 118, no. 10, p. 104801, Mar. 2017. doi: 10.1103/PhysRevLett.118.104801. <https://link.aps.org/doi/10.1103/PhysRevLett.118.104801>
- [8] Q. Gao *et al.*, “Observation of High Transformer Ratio of Shaped Bunch Generated by an Emittance-Exchange Beam Line,” *Phys. Rev. Lett.*, vol. 120, no. 11, p. 114801, Mar. 2018. doi: 10.1103/PhysRevLett.120.114801. <https://link.aps.org/doi/10.1103/PhysRevLett.120.114801>
- [9] G. Loisch *et al.*, “Observation of High Transformer Ratio Plasma Wakefield Acceleration,” *Phys. Rev. Lett.*, vol. 121, no. 6, p. 064801, Aug. 2018. doi: 10.1103/PhysRevLett.121.064801. <https://link.aps.org/doi/10.1103/PhysRevLett.121.064801>
- [10] A. Halavanau *et al.*, “Spatial control of photoemitted electron beams using a microlens-array transverse-shaping technique,” *Phys. Rev. Accel. Beams*, vol. 20, no. 10, p. 103404, Oct. 2017. doi: 10.1103/PhysRevAccelBeams.20.

103404. <https://link.aps.org/doi/10.1103/PhysRevAccelBeams.20.103404>
- [11] F. Lemery and P. Piot, "Tailored electron bunches with smooth current profiles for enhanced transformer ratios in beam-driven acceleration," en, *Physical Review Special Topics - Accelerators and Beams*, vol. 18, no. 8, p. 081301, Aug. 2015, ISSN: 1098-4402. DOI: 10.1103/PhysRevSTAB.18.081301. <https://link.aps.org/doi/10.1103/PhysRevSTAB.18.081301>
- [12] J.-L. Delcroix and A. R. Trindade, "Hollow Cathode Arcs," in *Advances in Electronics and Electron Physics*, L. Marton, Ed., vol. 35, Academic Press, Jan. 1974, pp. 87–190. DOI: 10.1016/S0065-2539(08)60281-4. <http://www.sciencedirect.com/science/article/pii/S0065253908602814>
- [13] G. R. Lynch and O. I. Dahl, "Approximations to multiple Coulomb scattering," en, p. 5.
- [14] Q. Gao *et al.*, "Single-shot wakefield measurement system," *Phys. Rev. Accel. Beams*, vol. 21, no. 6, p. 062801, Jun. 2018. DOI: 10.1103/PhysRevAccelBeams.21.062801. <https://link.aps.org/doi/10.1103/PhysRevAccelBeams.21.062801>
- [15] J. J. Yang, A. Adelman, M. Humbel, M. Seidel, and T. J. Zhang, "Beam dynamics in high intensity cyclotrons including neighboring bunch effects: Model, implementation, and application," *Phys. Rev. ST Accel. Beams*, vol. 13, no. 6, p. 064201, Jun. 2010. DOI: 10.1103/PhysRevSTAB.13.064201. <https://link.aps.org/doi/10.1103/PhysRevSTAB.13.064201>
- [16] M. Borland, *Elegant: A Flexible SDDS-Compliant Code for Accelerator Simulation*.